

Templating Organosilicate Vitrification using Unimolecular Self Organizing Polymers: Evolution of Morphology and Nanoporosity Development with Network Formation

*Ho-Cheol Kim, Teddie Magbitang, Victor Y. Lee, Robert D. Miller, Mike F. Toney,[‡]
Zhaoling Lin,⁺ Robert Briber,⁺ James L. Hedrick*

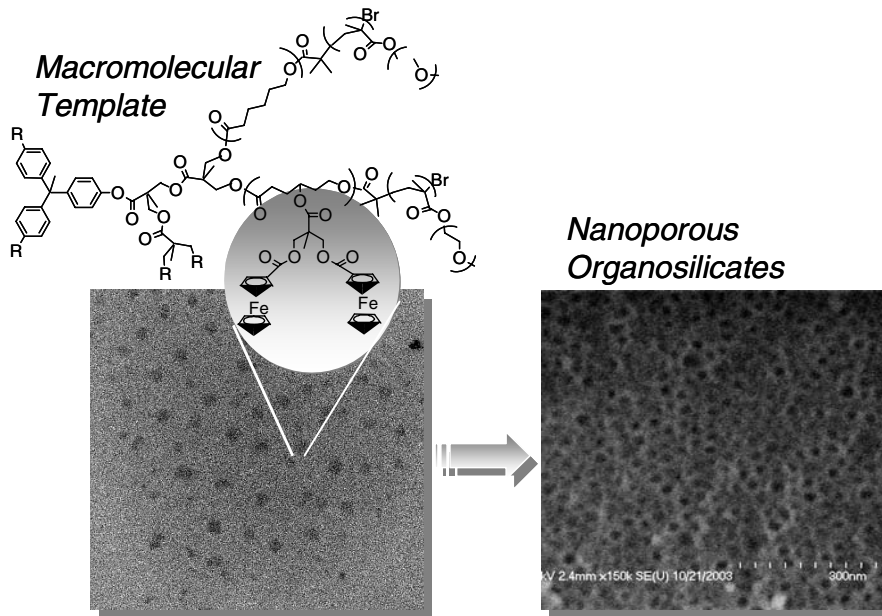
*IBM Almaden Research Center
650 Harry Rd
San Jose, CA 95120
Hedrick@almaden.ibm.com*

*[‡]SSL-Stanford Linear Accelerator Center,
2575 Sand Hill Road,
Menlo Park, CA 94025*

*⁺Department of Materials Science and Engineering
University of Maryland
College Park, MD 20742*

Abstract: Star-shaped polymers with a compatibilizing outer corona were dispersed into a thermosetting organosilicate matrix and used to create a nanoporous material. These environmentally responsive copolymers create nano-sized domains through a matrix-mediated collapse of the interior core of the core-corona polymeric structure. This approach relies on the outer corona of the star to compatibilize the insoluble core with the thermosetting resin and prevent aggregation such that these individual molecules template the crosslinking of the matrix and ultimately generate a single hole. The organic polymer was selectively thermalized leaving behind its latent image in the matrix with a pore size that reflected the size of the polymer molecule, and provided the expected reduction in dielectric constant. The morphology development as a function of arm number, molecular weight and volume fraction in mixtures with organosilicates as a function of cure/network conversion was investigated by SAXS, SANS, DMA, TEM and FE-SEM measurements. Amphiphilic star-shaped polymers of various block lengths and arm number, prepared by tandem controlled ring-opening polymerization (ROP) and atom transfer radical polymerization (ATRP) from dendritic initiators, were further tailored to facilitate contrast enhancement for various measurements by the incorporation of either ferrocenyl units or deuterated monomers. The pore sizes achieved by the star and dendrimer-like star macromolecular architectures range from ~7 to 40nm, depending on the molecular weight and architecture.

Graphical Abstract: The nanoporous precursor structures created by unimicellar star polymers in organosilicate thermosets produce morphologically controlled porous materials for semiconductor chip applications.



The semiconductor industry has historically experienced a two-fold increase in performance approximately every three years,¹ and for this trend to continue, revolutionary technologies and bottom-up design strategies will be required. As wiring and device densities continue to increase, lower dielectric constant insulating materials will be required to minimize signal delays and crosstalk. Clearly, dielectric constant values below 2.0 will require porosity, and to be useful for on-chip applications, the pores must be ~10X smaller than the smallest device features, approaching 100nm currently. Although there are numerous strategies to porous materials and interlayer dielectrics, few satisfy all the demanding requirements including pore size and minimal pore interconnectivity.² Recently, we have described an alternative approach to the generation of nanoporous materials using star-shaped amphiphilic copolymers that organize the organosilicate vitrificate into nanostructures.³ This approach relies on the outer corona of the star to compatibilize the insoluble core with the thermosetting resin and mitigate aggregation such that these individual molecules template the crosslinking of the matrix (vitrificate) and ultimately generate a single pore upon thermolysis. These unimolecular polymeric micelles do not show the complex dynamic assembly typical of most amphiphilic systems, adding to the ease of processing the hybrids into thin films. Moreover, unlike diblock templates that tend to organize polymerizing silica into contiguous nanostructures, this architecture minimizes such features due to the curvature constraints of the core. In our initial communication, we described the ruthenium-catalyzed ring-opening metathesis polymerization arm first approach to star-shaped amphiphilic polymers, where pore sizes were limited to 15-20nm and larger. To achieve a pore size of 10nm and below, a sacrificial template is required with a significantly lower molecular weight that retains its unique responsiveness to its environment. Towards this goal, we have explored core-out or bottom-up living polymerization routes to star-shaped and dendritic amphiphilic polymers from various generations of dendritic initiators.⁴ One objective is to understand the minimal molecular weight and architecture type required to maintain a self-organizing template motif (i.e., prevent dissolution of the pore-generating material in the organosilicate matrix followed by phase separation via nucleation and growth processes) while minimizing feature sizes. Another objective is to understand the

evolution of structure and porosity development as a function of cure/conversion with temperature.

The “organosilicate-phobic” core was based on an aliphatic polyester, poly(ϵ -caprolactone), prepared using a “bottom-up” or core-out approach to twelve and twenty-four arm star-shaped amphiphilic templates. The dendritic initiators used in this study are the second (G-2) and third generation (G-3) hydroxy functionalized bis-MPA dendrimers, generating twelve and twenty-four arm star polymers respectively from the ROP of either ϵ -caprolactone and derivatives or L-lactide in the presence of a catalytic amount of Sn(Oct)₂ in bulk (supplemental information), Table 1.⁴ The targeted degree of polymerization, DP, for each arm of the star polymers ranged from 10 to 50 and the average DP's, calculated by ¹H NMR, were comparable to the targeted values (Table 1). In addition to the poly(ϵ -caprolactone) stars (**2a-c**), polymers comprised of deuterated poly(ϵ -caprolactone), **2d-f**, and ferrocene-containing polyesters, **2g**, were also prepared. Introduction of initiating centers for ATRP at the chain ends of the star-shaped polycaprolactone was accomplished by esterification of the hydroxyl functional chain ends with 2-bromo-2-methylpropionyl bromide in THF in the presence of triethylamine (Scheme 2).^{4a} ATRP of poly(ethyleneoxy) methacrylate-functional macromonomers from the star-shaped macroinitiators was accomplished in solution at 85°C using NiBr₂(PPh₃)₂ as the organometallic promoter.⁵ The polymerizations were performed in toluene (20% solids) at 85°C in the presence of 20 mol.% catalyst for 18 hours. Reduced catalyst concentrations and diluted polymerization mixtures minimized intermolecular radical-radical coupling reactions.^{4a} The polymers were isolated in hexane, redissolved in THF and fractionally precipitated by the addition of hexane. This general ATRP procedure, with targeted DP's varying from ~20 to 40 for the outer corona (Table 2), was used to survey each of the macroinitiators.

It has been shown that these amphiphilic star-shaped and dendritic structures form unimolecular micelles in solution, which respond in a unique fashion to the polarity of solvent by changing their molecular geometry.^{4a,6} TEM microscopy of ultra thin films of copolymer **4g** (a 12-arm PCL core with an average DP of 50 per arm) (Table 2) deposited from water was used to investigate the responsiveness in a polar environment as well as

obtain an estimate of the size in the “dry” state. The contrast in the TEM micrograph of **4g**, resulting from the ferrocene functionality introduced into the PCL core, confirms the two phase structure containing a collapsed core with a diameter around 22nm and ~ 49nm spacing between the core centers (Figure 1). Alternatively, the size of the star polymers was determined in THF solution using Dynamic Light Scattering techniques (DLS) (Table 2). In solution, a single star-shaped polymer assumes a solvent-swollen state and hence the values obtained by DLS represent the upper limit in size. For example, the smaller star **4a** had a hydrodynamic diameter D_h of 13.2 nm while that of the larger star **4c** was 26.4 nm (measured in THF). Polymer **4g** has a D_h value of 26.0 nm that is consistent with the TEM measurements.

The amphiphilic copolymers were dissolved in a solution containing methyl silsesquioxane (MSSQ) prepolymer in propylene glycol monomethyl ether, and the resulting solution was spun on a silicon wafer to produce thin films that were cured to 430°C to effect network formation of the MSSQ and decomposition of the sacrificial copolymer template. The refractive indices of the samples decrease predictably from 1.36 to 1.26 and 1.21 with increasing copolymer loading (20 and 40%), respectively, and dielectric constants of 2.32 and 1.95 were measured for the latter samples, consistent with a porous structure. Shown in Figure 2 are the cross-sectional FESEM micrographs generated from hybrids containing 20 and 40 wt. % of **4c**, where the porous structure appears somewhat irregular at 20 % loading but becomes more evident and regular at the higher composition. Consistent with these data, TEM micrographs generated from hybrids containing 20 and 40 wt. % of **4a** (the lowest molecular weight copolymer template) show what appear to be a random porous morphology at the low composition and a significantly more ordered porous structure at the high template composition (Figure 3). Interestingly, the pore sizes generated from this template are in the single-digit nanometer range (~7-9 nm for the 20 wt% and around 9 nm for the 40 wt% copolymer template). Representative $\tan \delta$ curves obtained from Dynamic Mechanical Analysis (DMA) for **4b**/MSSQ hybrid (40 wt.% copolymer loading) after cure temperatures of 80°C (minimal advancement in MSSQ molecular weight), 150°C (partial cure/advancement in molecular weight of MSSQ) and 250°C (nearly complete cure or

network formation of MSSQ) are presented in Figure 4. Irrespective of the cure temperature and degree of network formation, a two phase structure is clearly evident (see shoulder on main $\tan \delta$ peak) even for the low temperature cure where the MSSQ exists as a prepolymer, and the observation of the T_g at -65°C is likely that the PCL phase, since it is immiscible with the MSSQ. This data suggest that the core is phase separated in the as-cast films and serves, as a macromolecular template, where one star generates one pore.

The small angle neutron scattering (SANS) of **4f** (Table 2), having a deuterated core for contrast (macroinitiator **2f**, Table 1), in mixtures containing 20 and 40wt.% copolymer with the MSSQ prepolymer are shown in Figure 5a and b, respectively, and confirm the phase separation of the PCL core upon film deposition. In particular, strong scattering intensity was observed for the 40 wt. % copolymer composition sample at a temperature of 40°C , indicating two-phase state of the mixture. Approximately same absolute scattering intensities were observed for 120°C and 250°C where porogen domains certainly exist within crosslinked MSSQ matrix. Further heating to 450°C removes the porogen creating porosity and the scattering intensity decreases significantly. Likewise, the hybrid sample containing 20 wt % copolymer shows similar, but much less well-defined behavior, consistent with the TEM and FESEM data. Nonetheless, the SANS data strongly support the fact that porogen molecules are phase-separated in the as-cast film and template porous structure.⁷

The microstructures of nanohybrid and porous films were also investigated using a small angle x-ray scattering (SAXS).⁸ Figure 6 a shows a SAXS profile of a mixture of MSSQ with **4g** (40 wt.% copolymer). The iron is necessary to provide contrast in the nanohybrid. The profile shows a strong peak in the low q region corresponding to the spacing between dispersed domains. The peak maximum is located at approximately $q_m=0.0224$ (\AA^{-1}), which gives the domain⁹ center-to-center spacing of 280\AA ($D=2\pi/q_m$). A number of additional broad scattering maxima were also observed at higher q , but the positions are somewhat unclear for this sample due to the noise in the data. Figure 7b shows a SAXS profile of porous MSSQ generated by 40 wt% of **4c**. It shows a strong

first scattering peak with a number of higher order scattering maxima caused by inter-pore interference, indicating that the spatial arrangement of the pores is regular. The pore spacing obtained from q_m is $\sim 310 \text{ \AA}$ for this sample. Two other broad scattering maxima marked by arrows can be attributed to the form factor. Assuming spherical pores, the scattering maxima give a radius of 75 \AA for **4c** and 39 \AA for **4a**, consistent with the pore sizes estimated from the TEM micrographs.

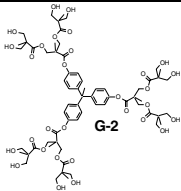
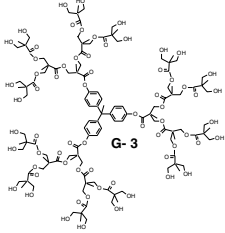
In summary, environmentally responsive star-shaped copolymers with a compatibilizing outer corona were used to organize the MSSQ vitrificate into nanostructures through a matrix-mediated collapse of the interior core. DMA, SANS and SAXA measurements strongly suggest that the core is phase separated in the as-cast films and serves, as a macromolecular template, where one star generates one pore. The porous morphology was strongly dependent on the arm number, molecular weight of the interior core as well as the volume fraction of copolymer in MSSQ mixtures. The bottom-up/core out approach to star porogens produced a porous structure with pores that range in size from 7 to 40nm, depending on polymer molecular weight and architecture.

Acknowledgements

The authors acknowledge support through the NSF Center for Polymer Interfaces and Macromolecular Assemblies (CPIMA: NSF-DMR-0213618). We also acknowledge the support of the National Institute of Standards and Technology, U.S. Department of Commerce, in providing the neutron research facilities used in this work.

This work utilized facilities supported in part by the National Science Foundation under Agreement No. DMR-9986442. The SAXS experiments were performed at the Advanced Photon Source at Argonne National Laboratory, which is supported by the U. S. Department of Energy, Office of Science, Office of Basic Energy Sciences, under Contract No. W-31-109-ENG-38.

Table 1. Characteristics of poly(caprolactone) star-shaped macroinitiators.

Sample Entry	Initiator	Targeted DP, M/I	DP ¹ H-NMR	Mw/Mn (PDI)	Mw (SEC)
2a		10	12	1.21	20,000
2b		20	17	1.12	34,000
2c		50	48	1.20	62,000
2d		10	11	1.21	24,000
2e		25	24	1.11	47,000
2f		50	48	1.46	69,000
2g		50	45	1.17	84,000
3a		25	24	1.18	70,000
3b		60	62	1.24	87,000

Comonomer used in **2g**

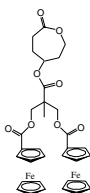


Figure Captions

Figure 1. TEM micrograph of copolymer **4g** deposited from water.

Figure 2. FESEM of MSSQ mixtures with **4c** at 20 and 40 wt. % copolymer.

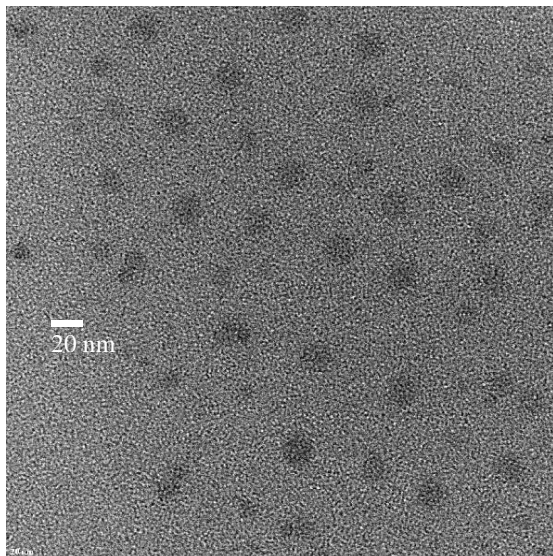
Figure 3. TEM micrographs of MSSQ mixtures with **4a** at 20 and 40 wt. % copolymer.

Figure 4. DMA chromatograms of MSSQ mixtures with **4b** at 20 and 40 wt. % copolymer.

Figure 5. Temperature dependent SANS profiles of MSSQ/**4f** nanohybrids. (a) 20% loading, (b) 40% loading.

Figure 6. (a) SAXS profile of MSSQ/**4g** 60/40 nanohybrid. (b) SAXS profile of porous MSSQ generated with 40% **4c**.

Figure 1. TEM micrograph of copolymer **4g** deposited from water.



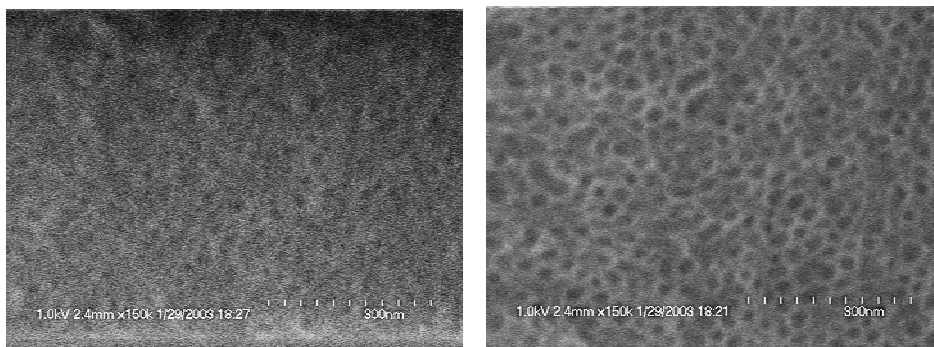


Figure 2. FESEM micrographs of MSSQ mixtures with **4c** at 20 and 40 wt. % copolymer.

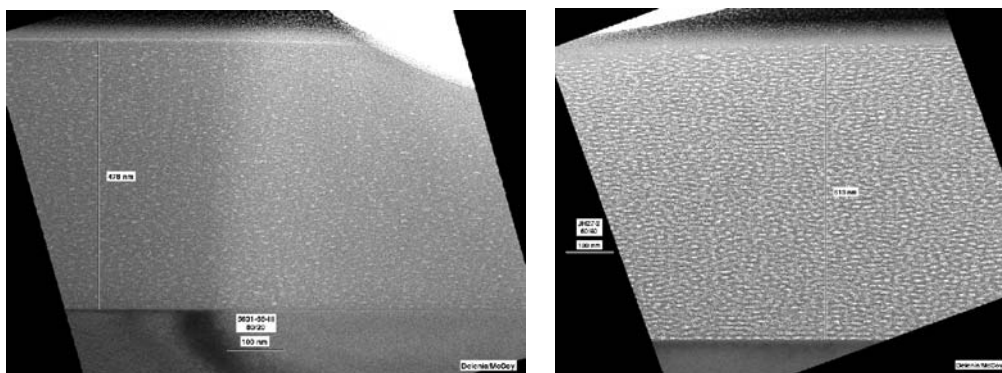


Figure 3. TEM micrographs of MSSQ mixtures with **4a** at 20 and 40 wt. % copolymer.

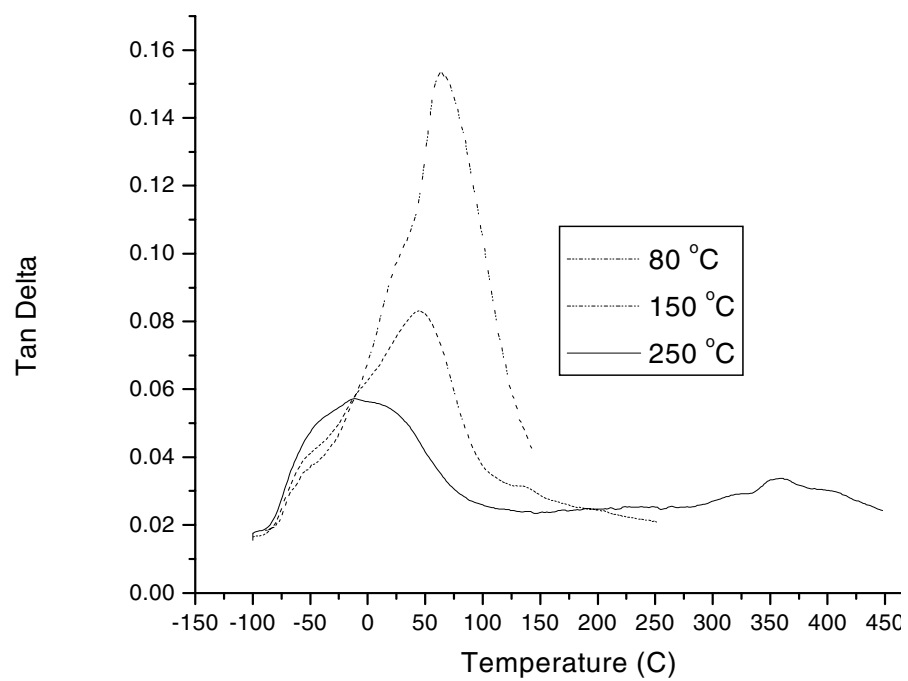


Figure 4. DMA chromatograms of MSSQ mixtures of **4b** at 20 and 40 wt. % copolymer.

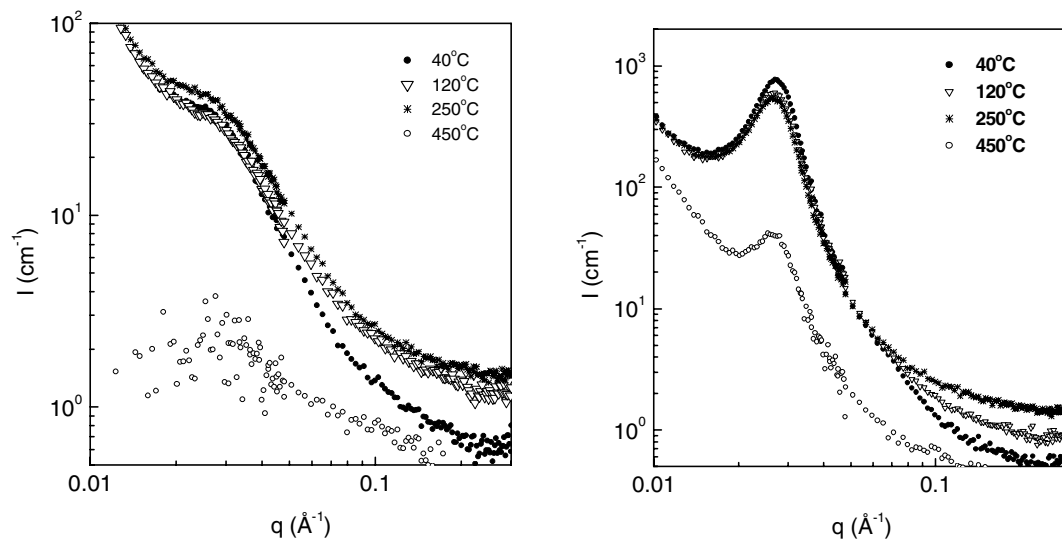


Figure 5. Temperature dependent SANS profiles of MSSQ/4f nanohybrids. (a) 20% loading, (b) 40% loading.

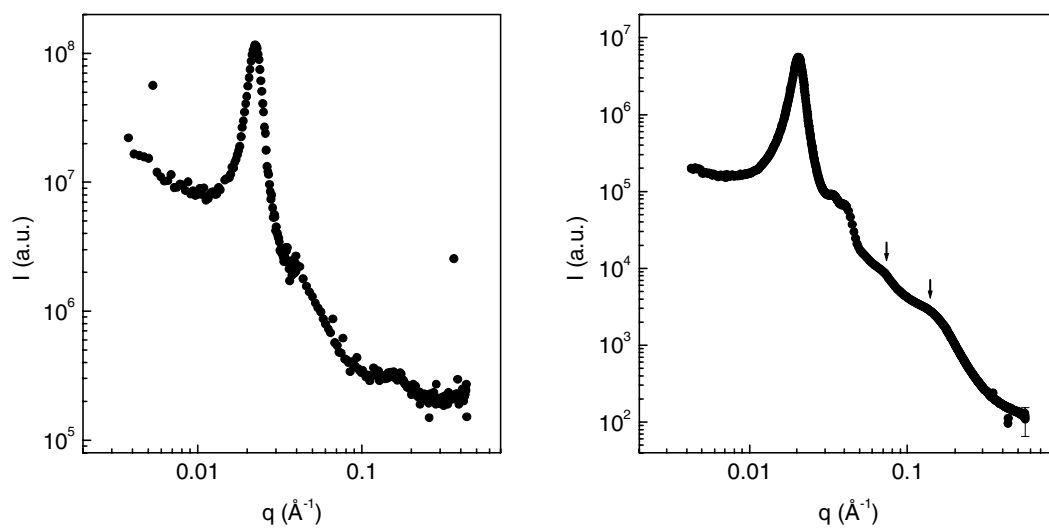
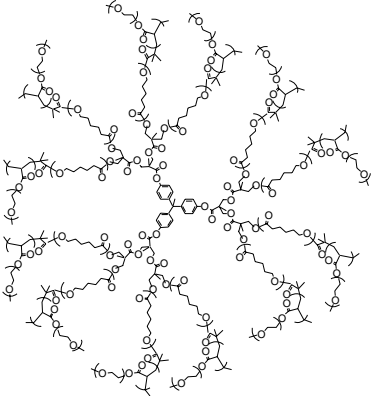


Figure 6. (a) SAXS profile of MSSQ/4g 60/40 nanohybrid. (b) SAXS profile of porous MSSQ generated with 40% 4c.

Table 2. Characteristics of amphiphilic radial block copolymers.



Sample Entry	Core	Shell Type	DP PEO (Shell)	Mw (SEC)	Mw/Mn PDI	D _n (DLS nm)
4a	2a	PEO	12	44,200	1.09	26.4
4b	2b	PEO	16	48,700	1.04	26.8
4c	2c	PEO	8	42,600	1.04	32.0
4d	2d	PEO	28	65,000	1.12	
4e	2e	PEO	32	81,000	1.11	
4f	2f	PEO	30	105,000	1.21	52.8
4g	2g	PEO	38	135,000	1.25	52.0
5a	3a	PEO	18	99,500	1.08	36.0
5b	3b	PEO	38	113,600	1.20	48.4

¹ The National Technology Roadmap for Semiconductors; Semiconductor Industry Association: San Jose, CA 1997.

² For example: D. L. Gin, W. Gu, B. A. Pindzola, W.-W. Zhou *Acc. Chem. Res.* **2001**, 34, 973. b) C. Yu, J. Fan, B. Tain, G. D. Stuck, D. Zhao *J. Phys. Chem. B* **2003**, 107, 13368. c) B.-H. Han, S. Poarz, M. Antonietti, *Chem. Mater.* **2001**, 13, 3915. d) M. Templin, A. Franck, A. Du Chesne, H. Leist, T. Ahang, R. Ulrich, V. Schadler, U. Wiesner, *Science* **1997**, 278, 1795. e) D. Zhao, J. Feng, Q. Huo, N. Melosh, G. H. Frederickson, B. F. Chmelka, G. D. Stucky *Science* **1998**, 279, 548. f) A. Okabe, T. Fukushima, K. Ariga, T. Aida *Angew. Chem. Int. Ed.* **2002**, 41, 3414. g) J. L. Hedrick, T. Magbitang, E. F. Connor, T. Glauser, W. Volksen, C. J. Hawker, V. Y. Lee, R. D. Miller, *Chemistry-a European Journal* **2002**, 8, 3308. h) Y. Chujo, H. Matsuk, S. kure, T. Saegusa, T. Yazawa *J. Chem. Soc., Chem Com.* **1994**, 635.

³ E. F. Connor, L. K. Sundberg, H.-C. Kim, J. J. Cornelissen, T. Magbitang, P. M. Rice, V. Y. Lee, C. J. Hawker, W. Volksen, J. L. Hedrick, R. D. Miller *Angew. Chem. Int. Ed.* **2003**, 42, 3785.

⁴ For example: a) J. L. Hedrick, M. Trollsas, C. J. Hawker, B. Atthoff, H. Claesson, A. Heise, R. D. Miller, *Macromolecules*, **1998**, 31, 8691. b) M. Trollsås, J. L. Hedrick, *J. Am. Chem. Soc.* **1998**, 120, 4644. c) M. Trollsås, H. Claesson, B. Atthoff, J. L. Hedrick, *Angew. Chem. Int. Ed. Engl.* **1998**, 37, 3132. d) Y. Gnanou, D. Taton, *Macromol. Symp.* **2001**, 174, 333. e) R. Knischka, P. Lutz, A. Sunder, R. Mulhaupt, H. Frey *Macromolecules* **2000**, 33, 315. f) V. Percec, B. Barboiu, C. Grigoras, T. K. Bera *J. Am. Chem. Soc.* **2003**, 125, 6503.

⁵ For example: a) K. Matyjaszewski, Ed., *ACS Symp. Series* **1998**, 685. b) T. E. Patten, Xia, J.; T. Abernathy, K. Matyjaszewski, *Science* **1996**, 272, 866; c) M. Kato, M. Kamigaito, M. Sawamoto, T. Higashimura, *Macromolecules* **1995**, 28, 1721. d) C. Granel, P. Dubois, R. Jérôme, P. Teyssié *Macromolecules* **1996**, 29, 8576. e) V. Percec, B. Barboiu, *Macromolecules* **1995**, 28, 7970. f) C. J. Hawker, A. N. Bosman, E. Harth *Chem. Rev.* **2001**, 101, 3661.

⁶ For example: a) I. Gitsov, J. M. J. Frechet *J. Am. Chem. Soc.* **1996**, 118, 3785. b) J. C. M. van Hest, D. A. P. Delnoye, M. W. P. L. Baars, M. H. P. van Genderen, E. W. Meijer *Science* **1995**, 268, 1592. c) A. Heise, J. L. Hedrick, C. W. Frank, R. D. Miller, *J. Am. Chem. Soc.* **1999**, 121, 8647. d) A. W. Bosman, H. M. Jansen, E. W. Meijer, *Chem. Rev.* **1999**, 99, 1665. e) S. Hecht, Fréchet, J. M. J. *Angew. Chem. Int. Ed.* **2001**, 40, 74 f) D. A. Tomalia, Dupont Durst, H. Topics in *Current Chemistry* **1993**, 165, 193. g) M. Antonietti, R. Basten, S. Lohmann, *Macromolecular Chemistry and Physics* **1995**, 196, 441; h) K. L. Wooley, *Journal of Polymer Science Part a-Polymer Chemistry* **2000**, 38, 1397. i) T. Glauser, C. M. Stancik, M. Moller, S. Voyteck, A. P. Gast, J. L. Hedrick *Macromolecules* **2002**, 35, 5774. j) A. Wursch, M. Moller, T. Gluser, L. S. Lim, S. B. Voytek, J. L. Hedrick, C. Frank, J. G. Hilborn *Macromolecules* **2001**, 34, 6601. k) J. Roovers, L. Zhou, P. M. Toporowski, M. van der Zwan, H. Iatrou, N. Hadjichristidis *Macromolecules* **1993**, 26, 4324. l) S. Liu, J. Weaver, M. Save, S. P. Arms *Langmuir* **2002**, 18, 8350.

⁷ J. S. Higgins, H. C. Benoit, *Polymers and Neutron Scattering*, Oxford University Press, **1994**.

⁸ E. Huang, M. Toney, W. Volksen, D. Mecerreyes, P. Brock, H.-C. kim, C. Hawker, J. L. Hedrick, V. Y. Lee, T. Magbitang, R. D. Miller, L. B. Luno, *Appl. Phys. Lett.* **2002**, 81, 2232.

⁹ D. J. Kinning, E. L. Thomas *Macromolecules* **1984**, 17, 1712.